MEMAT 2023: 9th International Conference on Mechanical Engineering, Materials and Automation Technology, 9-1 June 2023, Dalian, China.

Study on a NiTiHfTa shape memory alloy with high-pressure torsion and subsequent annealing

Zhang J T [a], Hu P [a], Wang S B [a], Zhang Y [b], Huang Y* [c,d], Ding H* [a,b]
[a] School of Materials Science and Engineering, Northeastern University, Shenyang 110819, China
[b] Key Laboratory of Light Structural Materials of Liaoning Province, Northeastern University, Shenyang 110819, China
[c] Department of Design and Engineering, Faculty of Science and Technology, Bournemouth University, Poole, Dorset BH12 5BB, UK
[d] Materials Research Group, Department of Mechanical Engineering, University of Southampton, Southampton SO17 1BJ, UK
[*] Corresponding author: yhuang2@bournemouth.ac.uk, dingh@smm.neu.edu.cn

ABSTRACT

An alloy with the composition of 49.6Ni-35.4Ti-9Hf-6Ta (at%) was processed by high-pressure torsion (HPT) and post-HPT annealing treatment. The microhardness of HPT-processed samples increased obviously, and amorphous feature appeared in 2 turns sample. The microhardness further increased and amorhozation was enhanced in 16 turns sample. After annealing at 750 ℃ for 3h, almost full crystallization occurs in 16 turns sample. In-situ high temperature X-ray diffraction experiment reveals that martensite to austenite transformation took place, indicating the alloy would exhibit SMA effect.

Keywords: NiTiHfTa, shape memory alloy, high-pressure torsion, annealing

1. INTRODUCTION

NiTi alloys possess good superelasiticity and shape memory effect as well as high corrosion resistance and have received much attention in research fields and industries [1]. Binary NiTi shape memory alloys (SMAs) are the most widely used and commercially available ones, but one disadvantage of these alloys is that their transformation temperatures are lower than 100℃, which limits their applications [2]. Recently, a lot of work has been done on the development of ternary Ni-Ti-Hf shape memory alloy as a high temperature SMA [3–7]. However, it was reported that the cold workability of Ni-Ti-Hf alloys is not good enough and the thermal stability of the alloys is not satisfying. Prasad et al designed a new high temperature NiTiHfTa SMA and characterized the microstructures and phase transformation behavior of the alloy [8].

Severe plastic deformation(SPD) has been introduced to SMAs to enhance the strength of the materials and shape memory effect as well [9–11]. Among SPD methods, high-pressure torsion (HPT) is the most efficient way to refine grain sizes of materials and has been utilized in tailoring the microstructures and properties of NiTiHf SMAs [12, 13]. However, there are no reports on the SPD work on NiTiHfTa alloys. In the present work, HPT and post-HPT annealing were applied on a NiTiHfTa alloy, and the microhardness was measured and phase constituents were characterized in order to provide experimental basis for tailoring microstructures of NiTiHfTa alloys.

2. EXPERIMENTAL

A NiTiHfTa ingot with a nominal composition of 49.6Ni-35.4Ti-9Hf-6Ta (at%) was prepared using a vacuum induction furnace. The ingot was subjected to homogenizing annealing at 1100℃ for 12 hr. The homogenized NiTiHfTa ingot is noted as the as-received material. The disk samples for HPT processing were cut by a wire cutting machine with 10 mm in diameter and 0.7~0.8mm in thickness. Pure Ti foils with a thickness of 0.1mm were cut into thin disks with a diameter of 10mm. One Ti foil disk was put on the top of the NiTiHfTa disk and the other Ti foil disk was put beneath the disk to form a sample with packed Ti, NiTiHfTa, Ti disks for HPT processing. The samples made up of packed disks were

processed by HPT up to 1/4, 2 and 16 turns at room temperature under a pressure of 4.0 GPa. The HPT-processed samples were annealed at 750℃ for 3h respectively and then water quenched.

Vickers microhardness of the NiTiHfTa alloy was measured by using a FM-700 tester. The load on the indenter was 0.5kg with a loading time of 10s. The microstructures of the samples were characterized by an OLYMPUS-DSX500 optical microscope and X-ray diffraction (X Pertpro, Cu-Ka radiation). And the sample subjected to HPT processing and post-HPT annealing were investigated by a Smart Lab 9Kw for in-situ high temperature diffraction. In-situ X-ray diffraction was used to study the martensitic transformation behavior of NiTiHfTa alloy, which revealed that it has good shape memory effect.

3. RESULTS AND DISCUSSION

3.1 As-received microstructure

The as received microstructure is shown in Figure 1 and lath-like structure is mainly martensite.

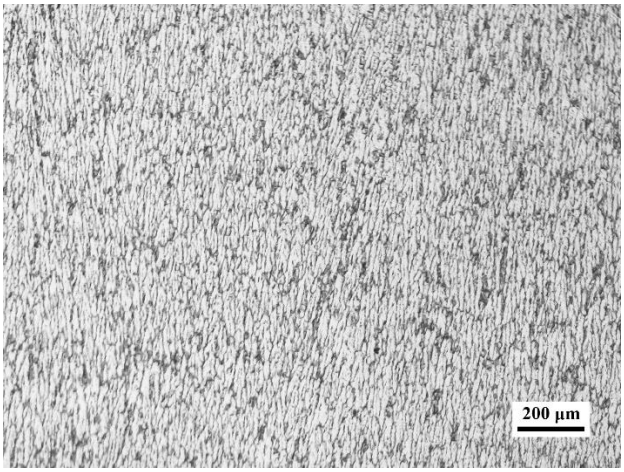

Figure 1 Optical microstructure of the as-received alloy

3.2 Microhardness analysis

Figure 2 shows the microhardness evolution from the as-received to the HPT-processed samples. HPT-processed samples exhibit a substantial increase in microhardness as compared with that of the as-received sample. It can be seen that the microhardness increases obviously in 1/4 turns sample and it doesn't change much when the number of turn increases from 1/4 to 2. The microhardness increases remarkably as the number of turn increase from 2 to 16. Measurements of the microhardness (Hv) distribution along radius in the HPT-processed samples show that Hv has the maximum value at the edge area and the minimum value in the center area of the samples. The increase in microhardness with the number of turn is resulted from gain refinement and the increased density of lattice defects during HPT [10]. Table 1 summarizes the microhardness results of different samples at the center, half-radius and edge areas.

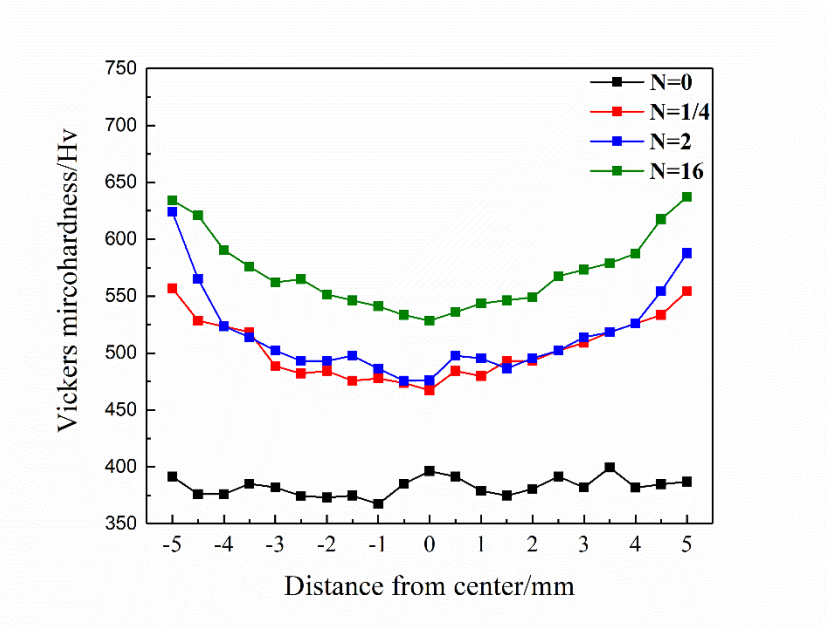

Figure 2. Microhardness distribution along diameter of the disks

Table 1. Microhardness of SMA samples at initial and deformed states

N	Microhardness （HV）		
	area		
	center	half-radius	edge
0	391.00±5.81	382.97±8.40	384.76±8.70
1/4	475.10±9.12	492.16±10.04	543.21±10.96
2	483.06±14.60	497.58±4.50	582.79±17.76
16	532.66±4.12	566.29±1.40	627.49±9.80

3.3 X-ray diffraction analysis

Figure 3 shows the XRD patterns of the as-received sample and HPT-processed sampels. The microstructure of as-received sample mainly consists of martensite and some austenite exists. XRD result shows that HPT leads to a broadening of martensite lines after 1/4 turn of HPT, resulting from the grain refinement. The half-width of $(100)_{B2}$ increases in 2 turns sample, which is an indication of the formation of amorphous phase. It is well known that cold SPD leads to the transition of the material into a non-equilibrium state due to the formation of densely populated lattice defects such as vacancies and dislocations [13]. The periodicity of atomic arrangement could be destroyed, and the formation of amorphous phase induced. Armophization has been reported in NiTi and NiTiHf SMAs during HPT [11, 12]. In the present HPT-processed NiTiHfTa alloy, the amorphous feature appears in 2 turns samples and the extent of armophization increases as the number of turns increases to 16.

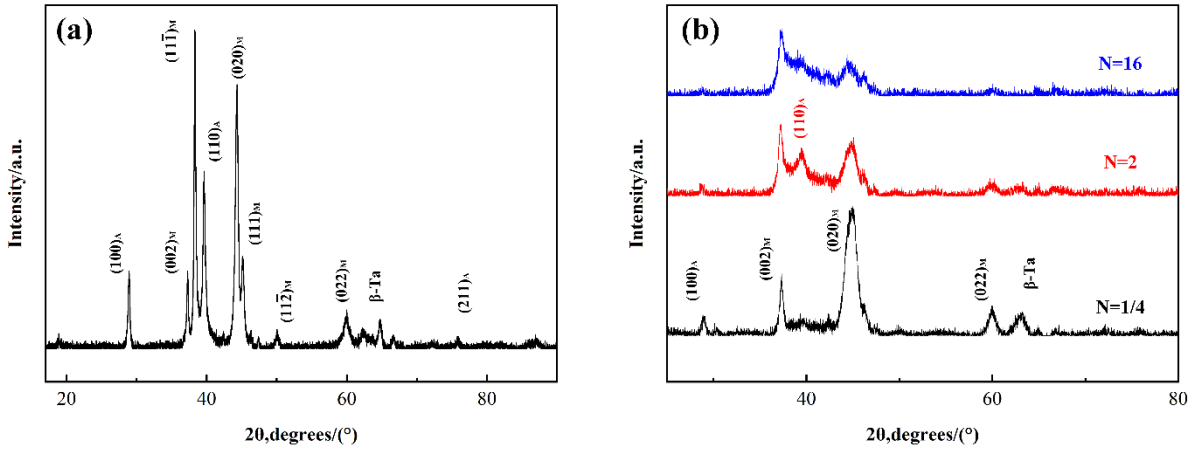

Figure 3. X-ray patterns of the (a) as-received and (b) HPT-processed samples

NiTi and NiTiHf alloys with amorphous structure after HPT can only exhibit SMA effect after crystallization in annealing [10, 11, 13]. From Fig.4, it can be seen that matensite is the major phase and some austenite coexists with marteniste in 16 turns sample after post-HPT annealing at 550℃ and 750℃ for 3 h, indicating that crystallization has occurred. The peak of β-Ta phase can also be seen. The results of in-situ XRD results are shown in Fig.5. Compared with the XRD result at room temperature (Fig.5(a)), the fraction of austenite increases obviously at the temperature of 400℃, with the newly formed (110) and (012) austenite peaks being quite high (Fig.5(b)), which reveals the occurrence of martensite to austenite phase transformation during the heating process and the NiTiHfTa alloy subjected to HPT and subsequent annealing could exhibit SMA effect. And with the increase of temperature, the fraction of austenite did not change significantly, which reveals that the transformation from martensite to austenite was basically completed at 150°C.

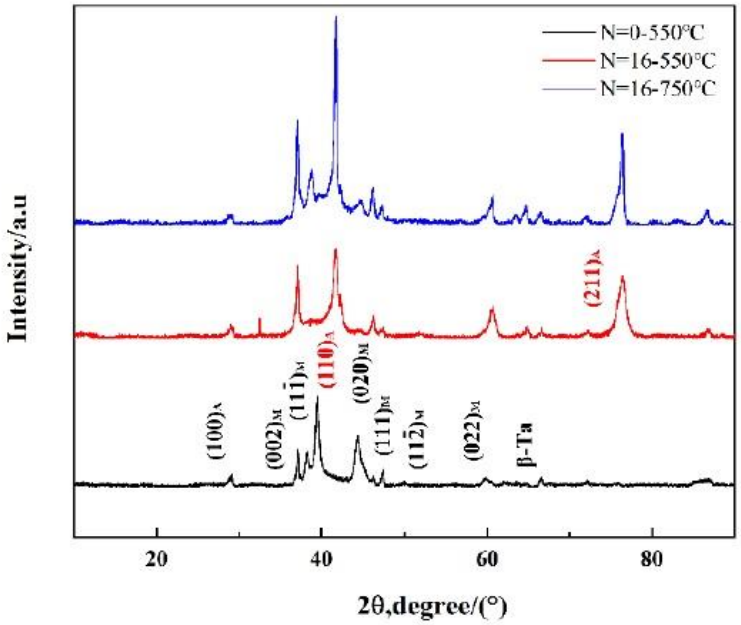

Figure 4. X-ray patterns of the samples with post-HPT annealing

Compared with the coarse grained SMA, the TiNi alloy with a ultrafine grained microstructure exhibits better properties such as better thermal cycling stability [14, 15], higher recovery strain and stress [16], lower stress hysteresis

and higher superelsticity [17] and higher radiation resistant capability [18] so that the application ranges of TiNi products could be enlarged. In severe plastic deformed TiNi and TiNiHf alloys, amorphous microstructures are generally attained and ultrafine microstructures could be achieved by post deformation annealing. Combining HPT and subsequent annealing treatments, one can tune the grain size and as a result the properties of the material can be controlled [11, 12]. The X-ray results mentioned above demonstrate that samples subjected to HPT processing and subsequent annealing underwent the processes of amorphization and crystallization. Therefore, it can be deduced that the processed quaternary 49.6Ni-35.4Ti-9Hf-6Ta (at%) alloy in the present work would exhibit good functional properties. Fine microstructure characterizations are in process.

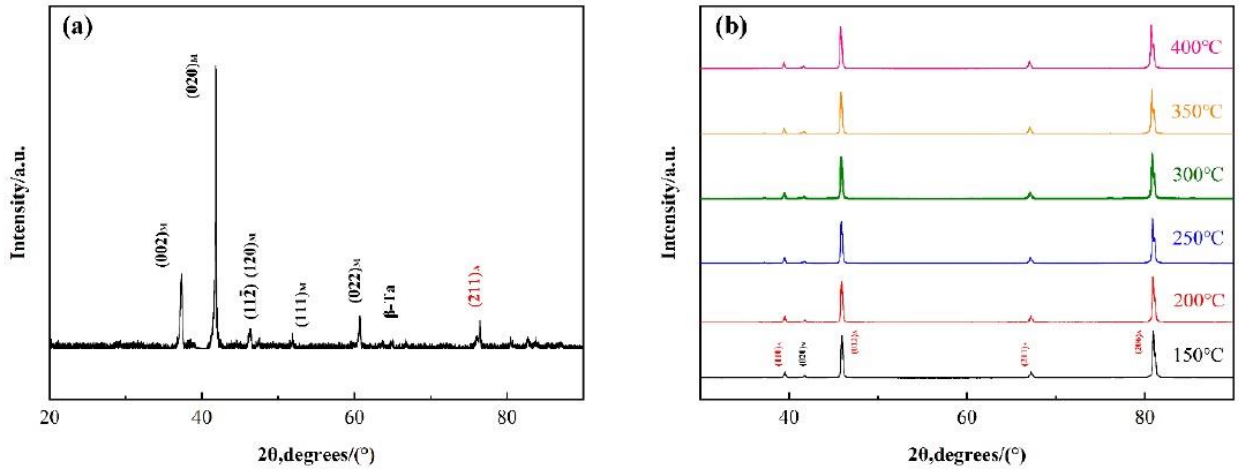

Figure 5. In-situ X-ray patterns of the HPT-processed sample (N=16) subjected to annealing (750℃/3h)

(a) room temperature; (b) heating up from 150℃ to 400℃

4. CONCLUSIONS

HPT and subsequent annealing treatment were applied to 49.6Ni-35.4Ti-9Hf-6Ta (at%) alloy. The microharness values of the samples after HPT increase substantially, especially in a large turn of 16. During HPT, amorphous phase appears after 2 turns of HPT processing and more amorphous phase forms as the number of HPT turns increases. To achieve a better crystallization effect, annealing at 750℃ was chosen in the 16 turns sample. In-situ X-ray diffraction at 150°C reveals the occurrence of martensite to austenite transformation, indicating that the alloy could exhibit SMA effect.

REFERENCES

[1] Mohd Jani, J., Leary, M., Subic, A., Gibson, M.A. (2014) A review of shape memory alloy research, applications and opportunities. Materials & Design (1980-2015). 56, 1078–1113. https://doi.org/10.1016/j.matdes.2013.11.084

[2] Chen, H., Xiao, F., Liang, X., Li, Z., Li, Z., Jin, X., Min, N., Fukuda, T. (2019) Improvement of the stability of superelasticity and elastocaloric effect of a Ni-rich Ti-Ni alloy by precipitation and grain refinement. Scripta Materialia. 162, 230–234. https://doi.org/10.1016/j.scriptamat.2018.11.024

[3] Saghaian, S.M., Karaca, H.E., Tobe, H., Turabi, A.S., Saedi, S., Saghaian, S.E., Chumlyakov, Y.I., Noebe, R.D. (2017) High strength NiTiHf shape memory alloys with tailorable properties. Acta Materialia. 134, 211–220. https://doi.org/10.1016/j.actamat.2017.05.065

[4] Karaca, H.E., Saghaian, S.M., Ded, G., Tobe, H., Basaran, B., Maier, H.J., Noebe, R.D., Chumlyakov, Y.I. (2013) Effects of nanoprecipitation on the shape memory and material properties of an Ni-rich NiTiHf high temperature shape memory alloy. Acta Materialia. 61, 7422–7431. https://doi.org/10.1016/j.actamat.2013.08.048

[5] Kockar, B., Karaman, I., Kim, J.I., Chumlyakov, Y. (2006) A method to enhance cyclic reversibility of NiTiHf high temperature shape memory alloys. Scripta Materialia. 54, 2203–2208. https://doi.org/10.1016/j.scriptamat.2006.02.029
[6] Hayrettin, C., Karakoc, O., Karaman, I., Mabe, J.H., Santamarta, R., Pons, J. (2019) Two way shape memory effect in NiTiHf high temperature shape memory alloy tubes. Acta Materialia. 163, 1–13. https://doi.org/10.1016/j.actamat.2018.09.058
[7] Toker, G.P., Nematollahi, M., Saghaian, S.E., Baghbaderani, K.S., Benafan, O., Elahinia, M., Karaca, H.E. (2020) Shape memory behavior of NiTiHf alloys fabricated by selective laser melting. Scripta Materialia. 178, 361–365. https://doi.org/10.1016/j.scriptamat.2019.11.056
[8] Prasad, R.V.S., Park, C.H., Kim, S.-W., Hong, J.K., Yeom, J.-T. (2017) Microstructure and phase transformation behavior of a new high temperature NiTiHf-Ta shape memory alloy with excellent formability. Journal of Alloys and Compounds. 697, 55–61. https://doi.org/10.1016/j.jallcom.2016.12.129
[9] Kockar, B., Karaman, I., Kim, J.I., Chumlyakov, Y. (2006) A method to enhance cyclic reversibility of NiTiHf high temperature shape memory alloys. Scripta Materialia. 54, 2203–2208. https://doi.org/10.1016/j.scriptamat.2006.02.029
[10] Valiev, R.Z., Gunderov, D.V., Lukyanov, A.V., Pushin, V.G. (2012) Mechanical behavior of nanocrystalline TiNi alloy produced by severe plastic deformation. J Mater Sci. 47, 7848–7853. https://doi.org/10.1007/s10853-012-6579-8
[11] Shahmir, H., Nili-Ahmadabadi, M., Huang, Y., Myun Jung, J., Seop Kim, H., Langdon, T.G. (2015) Shape memory effect in nanocrystalline NiTi alloy processed by high-pressure torsion. Materials Science and Engineering: A. 626, 203–206. https://doi.org/10.1016/j.msea.2014.12.056
[12] Ren, Y., Shuitcev, A., Gunderov, D.V., Li, L., Valiev, R.Z., Tong, Y.X. (2022) The role of temperature in the microstructural evolution of HPT-processed NiTiHf high-temperature shape memory alloy. Materials Letters. 322, 132484. https://doi.org/10.1016/j.matlet.2022.132484
[13] Shuitcev, A., Gunderov, D.V., Sun, B., Li, L., Valiev, R.Z., Tong, Y.X. (2020) Nanostructured Ti29.7Ni50.3Hf20 high temperature shape memory alloy processed by high-pressure torsion. Journal of Materials Science & Technology. 52, 218–225. https://doi.org/10.1016/j.jmst.2020.01.065
[14] Tong, Y.X., Guo, B., Chen, F., Tian, B., Li, L., Zheng, Y.F., Prokofiev, E.A., Gunderov, D.V., Valiev, R.Z. (2012) Thermal cycling stability of ultrafine-grained TiNi shape memory alloys processed by equal channel angular pressing. Scripta Materialia. 67, 1–4. https://doi.org/10.1016/j.scriptamat.2012.03.005
[15] Tong, Y.X., Chen, F., Guo, B., Tian, B., Li, L., Zheng, Y.F., Gunderov, D.V., Valiev, R.Z. (2013) Superelasticity and its stability of an ultrafine-grained Ti49.2Ni50.8 shape memory alloy processed by equal channel angular pressing. Materials Science and Engineering: A. 587, 61–64. https://doi.org/10.1016/j.msea.2013.08.049
[16] Prokofyev, E., Gunderov, D., Prokoshkin, S., Valiev, R. (2009) Microstructure, mechanical and functional properties of NiTi alloys processed by ECAP technique. In: European Symposium on Martensitic Transformations. p. 06028. EDP Sciences. https://doi.org/10.1051/esomat/200906028
[17] Tsuchiya, K., Hada, Y., Koyano, T., Nakajima, K., Ohnuma, M., Koike, T., Todaka, Y., Umemoto, M. (2009) Production of TiNi amorphous/nanocrystalline wires with high strength and elastic modulus by severe cold drawing. Scripta Materialia. 60, 749–752. https://doi.org/10.1016/j.scriptamat.2008.12.058
[18] Kilmametov, A.R., Gunderov, D.V., Valiev, R.Z., Balogh, A.G., Hahn, H. (2008) Enhanced ion irradiation resistance of bulk nanocrystalline TiNi alloy. Scripta Materialia. 59, 1027–1030. https://doi.org/10.1016/j.scriptamat.2008.06.051